How exceptional was the 2015–2019 Central American Drought?

Talia G. Anderson[1], Karen A. McKinnon[2], Diego Pons[3], Kevin J. Anchukaitis[1]

[1]School of Geography, Development and Environment, University of Arizona, Tucson, AZ
[2]Departments of Statistics and Data Science, and Atmospheric and Oceanic Sciences, and Institute of the Environment and Sustainability, University of California, Los Angeles, Los Angeles, CA
[3]Department Geography & the Environment, University of Denver, Denver, CO

Key Points:

- The 2015-2019 drought was severe, but it falls within the range of natural climate variability
- July-August deficits were the most significant drivers of overall drought
- Positive Caribbean Low-Level Jet anomalies are strongly associated with regional precipitation deficits

Corresponding author: Talia Anderson, `taliaanderson@arizona.edu`

Abstract

The Central American Dry Corridor experienced five consecutive years of drought from 2015 to 2019. Here, we find that the severity of this drought was driven primarily by rainfall deficits in July-August. To determine if the magnitude of this event was outside the range of natural variability, we apply a statistical resampling method to observations that emulates internal climate variability. Our analyses show that droughts similar to the 2015-2019 event are possible, although extremely rare, even without anthropogenic influences. Persistent droughts in our ensemble are consistently linked to positive anomalies of the Caribbean Low-Level Jet. We also examine the effects of temperature on soil moisture during this drought using the Palmer Drought Severity Index and show that anthropogenic warming increases the likelihood of severe deficits. Multi-year droughts are likely to worsen by the end of the 21^{st} century due to the compound effects of anthropogenic climate change.

Plain Language Summary

Climate models project that Central America is one of the global hotspots for future decreases in precipitation as a result of human-caused climate change. This is particularly concerning for the Dry Corridor region, which is already prone to frequent droughts and high levels of food insecurity among households. Much of this region experienced severe rainfall deficits between 2015-2019, provoking the question of whether or not this drought was caused by climate change or if it could have occurred because of natural climate variability alone. Using a statistical model, we show that while 2015-2019 was the driest period in the observational record, droughts as bad as this one are possible even without the influence of human-caused climate change. We also examine the additional role of temperature since it can modulate drought severity through its influence on soil moisture. We find warming temperatures increase the occurrences of greater soil moisture deficits. We also determine that the strength of the Caribbean Low-Level Jet, which transports moisture from the Caribbean Sea into Central America, is strongly associated with persistent dry conditions in the region.

1 Introduction

Five years of drought affected much of Central America from 2015 to 2019. Such multi-year events are a challenge for the millions of households that rely on rainfall for subsistence agriculture across the region (Morton, 2007; Hannah et al., 2017). This drought was particularly acute in the Central American Dry Corridor (CADC) – a region that already receives less rainfall than the rest of Central America and includes agricultural areas in Guatemala, El Salvador, Honduras, and Nicaragua (FAO, 2015; Gotlieb et al., 2019). Reports from 2018 and 2019 indicate widespread crop losses throughout the CADC (UN, 2018; FAO, 2018; WFP, 2019).

While Central America is among the regions expected to be most exposed to future drying due to anthropogenic climate change (Cook et al., 2020), it is uncertain when decreases in rainfall will become detectable beyond the range of natural climate variability (Almazroui et al., 2021). Irrespective of future emissions scenario, models consistently project that precipitation in the region will decline by the end of the century in nearly all seasons; however, only the high-end SSP5-8.5 scenario suggests significant decreases beyond natural variability in the upcoming decades (Almazroui et al., 2021). Due to observational and modeling uncertainties, the 2015-2019 drought provokes questions about the possible role of anthropogenic climate change and whether the drought was already outside the range of natural climate variability (Pascale et al., 2021; Depsky & Pons, 2020).

Understanding the full range of internal climate variability is therefore critical, as it has the potential to cause multidecadal unforced trends and extended dry and wet periods even in the absence of human-caused climate change (Deser et al., 2014; Deser, 2020;

McKinnon & Deser, 2021). This is known to be true for Central America and the Caribbean, which have experienced protracted wet and dry events linked to large-scale modes of ocean-atmosphere variability over the last several centuries (Hastenrath & Polzin, 2012; Anchukaitis et al., 2015; Jones et al., 2016; Hidalgo et al., 2019). Since limited instrumental observations (Giannini et al., 2001; Jones et al., 2016) preclude our ability to fully characterize the range of natural variability, initial condition large ensembles are a valuable climate modeling tool (Mankin et al., 2020; Deser, 2020). Using a climate model large ensemble approach, Pascale et al. (2021) evaluated the 2015-2019 Central American drought and recent trend in rainfall to determine possible contributions of anthropogenic climate change. They concluded that recent trends cannot be attributed to climate change, but that the likelihood of drought events like that of 2015-2019 has increased due to anthropogenic climate change (Pascale et al., 2021).

While large ensembles are invaluable tools for characterizing internal variability and evaluating future changes (Mankin et al., 2020), general circulation models often suffer in their ability to accurately represent regional climate variability (Thompson et al., 2015; McKinnon & Deser, 2021). This is particularly true for climate model representations of Central American precipitation (Karmalkar et al., 2011; Cavazos et al., 2020; Almazroui et al., 2021). For example, CESM1 does not reproduce the Central American Midsummer Drought (Pascale et al., 2021), an important period of reduced convective activity during the rainy season (Magaña et al., 1999).

As an alternative approach to evaluate the 2015-2019 meteorological drought in the CADC, we adopt the Observational Large Ensemble (OLEns) method originally developed by McKinnon et al. (2017). Using historical observations as the base for a statistical model, the OLEns preserves characteristics of regional climate that general circulation models may be unable to represent and provides a complement to large ensemble climate models for evaluating internal variability (McKinnon et al., 2017; McKinnon & Deser, 2018, 2021). This approach is advantageous since natural variability is one of the greatest sources of uncertainty in regional climate projections for the upcoming decades (Thompson et al., 2015; Lehner et al., 2020). Similar to Pascale et al. (2021), we focus primarily on precipitation due to the observed rainfall deficit during the 2015-2019 period and the role it played in causing meteorological drought. However, we also address calls to consider the potential role of anthropogenic warming (Aguilar et al., 2005; Pascale et al., 2021; Stewart et al., 2021) on this drought through an analysis of the Palmer Drought Severity Index (PDSI). PDSI mimics land-atmosphere interactions that allow it to serve as an indicator of soil moisture and agricultural drought (van der Schrier et al., 2013; Cook et al., 2018).

2 Methods

2.1 Observational data

We use monthly 0.5º Global Precipitation Climatology Centre (GPCC) data from 1920-2019 (Schneider et al., 2020) to characterize regional precipitation patterns and as the base of the OLEns. We select GPCC versus other datasets because of its length and more comprehensive station network, albeit still limited in the CADC (Schneider et al., 2017; Stewart et al., 2021; Jones et al., 2016). To be consistent with previous studies (Pascale et al., 2021), we focus on the drought between 2015-2019, although parts of the CADC suffered dry conditions as early as 2014 (CONASAN, 2014; OCHA, 2017). To assess the role of temperature in the 2015-2019 drought, we use the monthly self-calibrating 0.5º Climatic Research Unit (CRU) Palmer Drought Severity Index (PDSI) from 1940-2019 (van der Schrier et al., 2013; Barichivich et al., 2022). The PDSI dataset is derived from CRU-TS precipitation and temperature data (van der Schrier et al., 2013; Barichivich et al., 2022). We limit the GPCC and CRU datasets to 1920-2019 and 1940-2019, respectively, to avoid changes in variance that are likely artefact of limited observations in the earlier part of each product (Beguería et al., 2016). We subset both datasets to 11-18$^{\mathrm{o}}$N and 93-83$^{\mathrm{o}}$W and only include areas where >75% of annual rainfall occurs between May-October, which is indicative of areas with both a distinct rainy season (**Figure 1a**) and Midsummer Drought (Magaña et al., 1999; Anderson et al., 2019). Our study area approximates other delineations of the CADC (Maurer et al., 2017; Anderson et al., 2019; Gotlieb et al., 2019; Maurer et al., 2022), and does not include much of the Caribbean coast, which is characterized by a different precipitation regime and distinct associations to large-scale modes of climate variability (Magaña et al., 1999; Alfaro, 2000; Taylor & Alfaro, 2005; Karnauskas & Busalacchi, 2009). Following McKinnon and Deser (2021) (herein referred to as MD2021), we transform the GPCC observations with a Box-Cox power transform prior to fitting the OLEns model to reduce the influence of outliers and to prevent the model from generating negative precipitation amounts (Box & Cox, 1964).

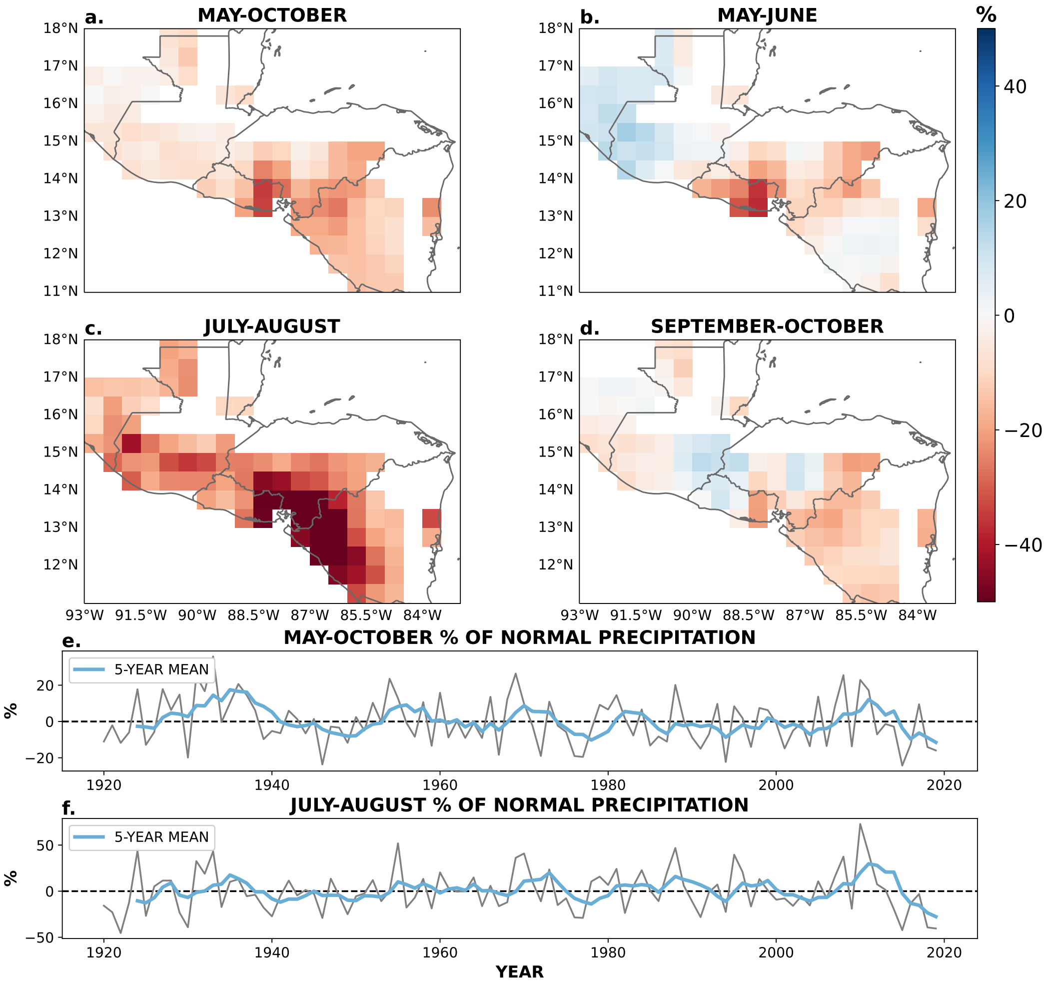

Figure 1. 2015-2019 precipitation % anomalies for **(a)** May-October, **(b)** May-June, **(c)** July-August, and **(d)** September-October. Study area includes grids where May-October precipitation is >75% of total annual precipitation. **(e)** Regionally averaged May-October precipitation based on % anomalies. **(f)** Regionally averaged July-August precipitation based on % anomalies.

The El Niño Southern Oscillation (ENSO) and Atlantic Multidecadal Variability (AMV) time series used in the OLEns are the same as those used in McKinnon and Deser (2018). ENSO is represented by the Niño3.4 Index calculated from the HadISST dataset

(Rayner et al., 2003) and the AMV is the average North Atlantic sea surface temperatures (SSTs) from 0-80ºN from the Kaplan SST dataset (Kaplan et al., 1998). The NCEI Pacific Decadal Oscillation (PDO) index is used, as it spans the full time period for in this analysis (Mantua & Hare, 2002; Huang et al., 2017). Due to the correlation between ENSO and the PDO, we follow MD2021 and orthogonalize the PDO index to the ENSO index for statistical independence. The Caribbean Low Level Jet (CLLJ) is defined as average 925 millibar winds over 12.5-17.5ºN and 80-70ºW (Wang, 2007). In order to generate a time series that matches the length of the GPCC data, we combine two datasets: NOAA/CIRES/DOE 20th Century Reanalysis (V3) from 1920-1948 with latitudes 12-18ºN based on the pre-defined coordinates and the IRI CLLJ Index from 1949-2019, which is based on NCEP/NCAR Reanalysis data (Kalnay et al., 1996). We do not orthogonalize the CLLJ to ENSO due to their relatively weak correlation ($r = 0.11$).

2.2 Synthetic Observational Large Ensemble

Generating the OLEns involves two main steps: (1) fitting a linear model to monthly average climate variables (here, either precipitation or the PDSI) and then (2) using this model to produce realistic synthetic spatiotemporal fields based on emulated internal variability. The linear model for precipitation is described by (1) the mean state, (2) the response to large-scale modes of climate variability including ENSO, CLLJ, PDO, and AMV, and (3) the residual stochastic variability at individual grid points:

$$P^{i,t} = \beta_0^{i,m(t)} + \beta_{ENSO}^{i,m(t)} ENSO^t + \beta_{CLLJ}^{i,m(t)} CLLJ^t + \beta_{AMV}^{i,m(t)} AMV^t + \beta_{PDO}^{i,m(t)} PDO^t + \epsilon^{i,t} \quad (1)$$

In equation 1, t is time, *m(t)* is the month, and i represents the geographic location. β_0 is the mean state of the climate variable and the other β coefficients describe the monthly sensitivity of P, the transformed precipitation, to the large-scale climate modes of ENSO, CLLJ, AMV, and PDO. ϵ describes the residual climate 'noise'. The MD2021 OLEns was designed to be applicable across global regions so did not include the CLLJ, but we incorporate it here due to its relevance to Central American precipitation dynamics (Wang, 2007; Taylor et al., 2013; Hidalgo et al., 2015, 2019; Anderson et al., 2019; García-Martínez & Bollasina, 2020). Similar to MD2021, we do not include the forced component in the precipitation OLEns for Central America since a forced signal in rainfall trends is not yet evident regionally (Pascale et al., 2021) and is not expected to emerge until the latter half of the 21^{st} century (Depsky & Pons, 2020; Almazroui et al., 2021). We herein refer to the ensemble of simulated historical precipitation as the prec-synth-OLE.

Since an anthropogenically forced signal has been observed in PDSI (Herrera et al., 2018), we add a term to equation 1 for the PDSI OLEns that represents the sensitivity of PDSI to forcing ($\beta_F^{i,m(t)} F^t$). Similar to MD2021, we define F^t as the Coupled Model Intercomparison Project (CMIP6) multi-model ensemble mean of monthly global average temperatures, combining the historical and SSP2-4.5 scenarios (Eyring et al., 2016; O'Neill et al., 2016; Dai et al., 2015). Shared Socioeconomic Pathways (SSP) emissions scenarios do not substantially diverge until later in the century, but SSP2-4.5 represents a "middle-of-the-road" emissions pathway (Masson-Delmotte et al., 2021; O'Neill et al., 2016). To isolate the influence of warming, we generate two PDSI OLEns. We herein refer to these ensembles of simulated historical PDSI as the forced and unforced pdsi-synth-OLE, respectively. Both include the forced term when fitting the linear model, but we remove the forcing term when generating the synthetic time series for the unforced pdsi-synth-OLE.

After fitting the linear model to the observational climate data, we follow MD2021 to create unique possible realizations of the climate variables by randomizing the large-scale climate modes and residuals as described below. Multiple versions of the ENSO, CLLJ, PDO, and AMV time series are produced through an Iterative Amplitude Adjusted Fourier Transform (IAAFT) method that retains the original amplitude distributions and power spectra (Schreiber & Schmitz, 1996). The IAAFT method does not preserve correlations between modes. The synthetic residual noise ($\epsilon^{i,t}$) spatiotemporal fields are generated through a block-bootstrapping approach, where the fields are resampled with replacement using a multiyear block size following Wilks (1997), allowing the OLEns to maintain a similar temporal autocorrelation to the original data. Following MD2021, we use the 97th percentile of all estimated block sizes for calculations to preserve the spatial correlation structure of the data; the block sizes in our study are 4 years for precipitation and 6 years for PDSI. The synthetic climate mode time series and residual fields are then linearly combined to produce pseudo climate histories of the original climate variables. Our full OLEns repeats this process 1,000 times.

We compare the 2015-2019 5-year mean of the observed climate variables and large-scale climate modes against the 5-year means across all 1,000 prec-synth-OLE and pdsi-synth-OLE members. We also evaluate the 40-year trends in the precipitation and PDSI observations and all prec-synth-OLE and pdsi-synth-OLE members using the non-parametric Mann–Kendall test with the Theil–Sen slope estimator (Yue & Wang, 2002; Hussain & Mahmud, 2019).

3 Results & Discussion

3.1 Characterization of the 2015-2019 Drought

We find that the 2015-2019 regional mean 5-year May-October precipitation was 11.49% below average (**Figure 1e**) with negative anomalies covering nearly the entirety of the region (**Figure 1a**). While this was the driest 5-year May-October period in the GPCC record, it only slightly surpassed the next driest period of 1974-1978. Analysis of the bi-monthly periods however reveals that July-August experienced the most significant decreases in rainfall and that deficits during this time were the primary driver of the overall seasonal drought. The 2015-2019 July-August regional mean surpassed all other 5-year means from outside of that time period by 13.72% (**Figure 1f**), with local negative precipitation anomalies ranging from approximately -63% to -8% of normal (**Figure 1c**). Since July-August is already a period of reduced rainfall due to the Central American Midsummer Drought, enhanced deficits in this period are particularly detrimental to crops yields (Magaña et al., 1999; Van der Zee Arias et al., 2012; Anderson et al., 2019). The May-June and September-October periods show more variable precipitation anomalies between 2015-2019 (**Figure 1b,d**) and are therefore not the focus for the following analyses.

Comparisons between the 5-year May-October and July-August mean precipitation observations and all 5-year periods from the prec-synth-OLE reveal that the 2015-2019 drought was indeed an extremely rare event, but did not fall outside the range of natural climate variability produced by the OLEns (**Figure 2a,b**). Only 1.42% of all 5-year May-October means from the prec-synth-OLE fall below the observed May-October mean (**Figure 2a**). When considering the full rainy season, the strongest deficits were concentrated in El Salvador and along the border between Honduras and Nicaragua (**Figure 3a**). The prec-synth-OLE demonstrates potential spatial variability among droughts at least as dry as 2015-2019, with some synthetic droughts comparable to the recent observed event and others with a similar overall regional deficit but varying spatial patterns (**Figure S1**). The observed July-August mean was even more exceptional (0.1 percentile) in the prec-synth-OLE context, with only 135 out of 96,000 possible 5-year drought events across the 1,000 ensemble members having an equal or greater magnitude than the observational drought (**Figure 2b**). The deficits were widespread regionally and the observational drought was below the 5th percentile of the prec-synth-OLE in 68% of grids (**Figure 3b**). An additional test in which we excluded the 2015-2019 precipitation data when fitting the climate mode β values and generating the $\epsilon^{i,t}$ fields for the prec-synth-

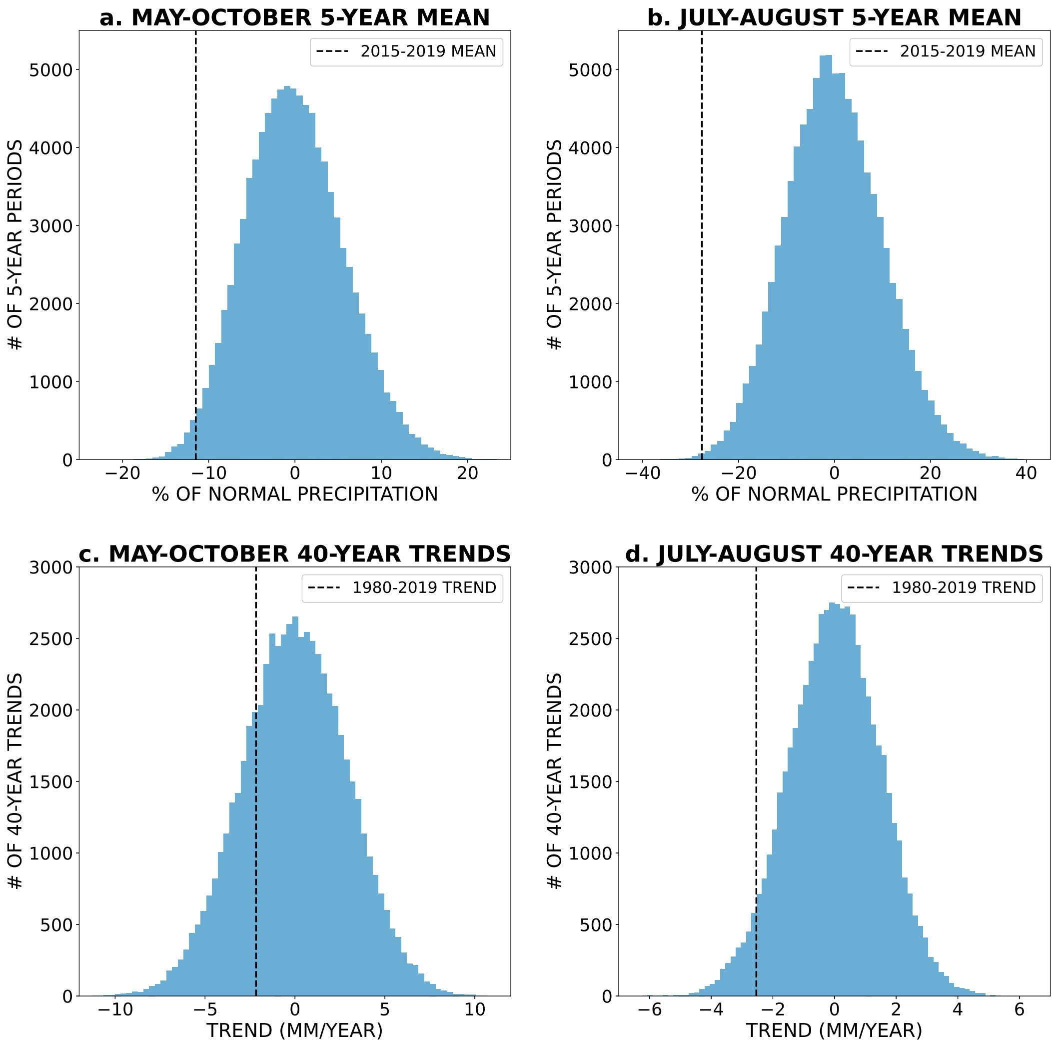

Figure 2. **(a)** Distribution of all regional average 5-year May-October precipitation anomalies from the prec-synth-OLE and the 2015-2019 May-October observational anomaly. **(b)** Distribution of all regional average 5-year July-August precipitation anomalies from the prec-synth-OLE and the 2015-2019 July-August observational anomaly. **(c)** Distribution of all possible regional 40-year trends in May-October precipitation (mm/year) from the prec-synth-OLE and the 1980-2019 regional May-October observational trend. **(d)** Distribution of all possible regional 40-year trends in July-August precipitation (mm/year) from the prec-synth-OLE and the 1980-2019 regional July-August observational trend.

OLE produced similar results, but with slightly more extreme July-August deficits where only 26 of 91,000 possible events were drier. These results highlight that this drought was extremely unusual, but that such a drought is still possible even without the additional influence of anthropogenic climate change.

Similar to the 2015-2019 drought event, we find that the observed 40-year precipitation trends are possible without the influence of anthropogenic climate change. Although both regional May-October (**Figure 2c**) and July-August (**Figure 2d**) precipitation trends are slightly negative, they are well within the natural variability in the prec-synth-OLE. This conforms with modeling results from Pascale et al. (2021) and regional

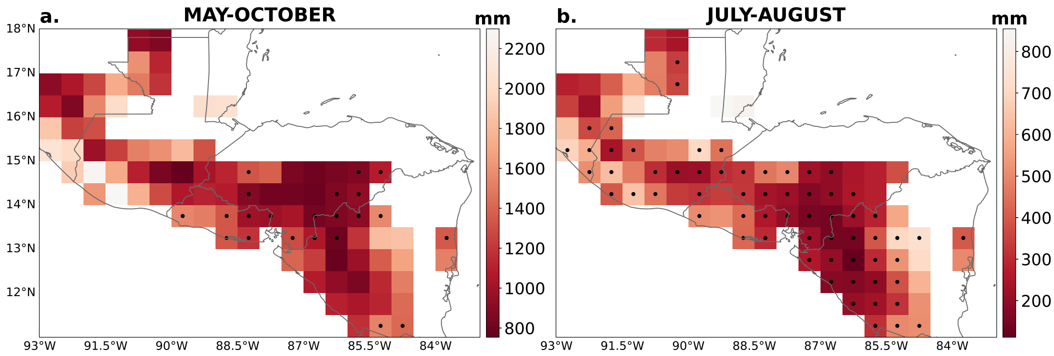

Figure 3. **(a)** 5^{th} percentile of all prec-synth-OLE 5-year May-October rainfall means (mm). Dots represent where the 2015-2019 May-October observed mean is less than the 5^{th} percentile of all prec-synth-OLE members. **(b)** 5^{th} percentile of all prec-synth-OLE 5-year July-August rainfall means (mm). Dots represent where the 2015-2019 July-August observed mean is less than the 5^{th} percentile of all prec-synth-OLE members.

analyses from instrumental and satellite-based observations, reanalysis products, and paleoclimate reconstructions, which do not reveal consistent trends in rainfall in terms of direction and/or magnitude over recent decades (Aguilar et al., 2005; Anchukaitis et al., 2015; Anderson et al., 2019; Muñoz-Jiménez et al., 2019; Stewart et al., 2021). The lack of coherent observed trends in regional Central American precipitation is very likely in part due to the continued dominance of a wide range of internal climate variability across spatial and temporal scales (Hastenrath & Polzin, 2012; Anderson et al., 2019; Muñoz-Jiménez et al., 2019; Hidalgo, 2021; McKinnon & Deser, 2021). However, more localized analyses reveal that some areas may already be experiencing significant changes in rainfall (Anderson et al., 2019; Cavazos et al., 2020; Stewart et al., 2021) and there is strong agreement across climate model simulations for declines in precipitation across Central America by the end of the 21^{st} century (Rauscher et al., 2008, 2011; Cook et al., 2020).

3.2 Climate Influences

Analysis of the 5-year mean climate mode values shows that the observed 2015-2019 drought occurred during positive phases of the CLLJ and ENSO (**Figure 4a,b**). Negative precipitation anomalies in our study region can occur in the rainy season during the development of a strong El Niño event due to a weaker and more southward displaced Inter-Tropical Convergence Zone (ITCZ) (Giannini et al., 2000; Karnauskas & Busalacchi, 2009). Regional rainfall deficits may persist as long as the ITCZ remains equatorward due to warmer equatorial sea surface temperatures (SSTs) (Karnauskas & Busalacchi, 2009). However, the sign of the ENSO influence on rainfall in the region is spatially and temporally variable over the lifecycle of an El Niño event (Giannini et al., 2000; Karnauskas & Busalacchi, 2009). Indeed, the β_{ENSO} coefficients from the OLEns model highlight the varying sign and magnitude of the ENSO-precipitation relationship across the CADC (**Figure S2**). Nevertheless, **Figure 4** shows that ENSO anomalies tend toward warmer mean conditions for the driest 5% of the precipitation prec-synth-OLE 5-year means, but can be associated with both warm and cool mean SST anomalies. This is consistent with Muñoz-Jiménez et al. (2019), who found that warm ENSO events are not always associated with rainfall deficits.

The relationship between rainfall deficits and the CLLJ, however, is more tightly coupled in the prec-synth-OLE, where dry periods are most often linked to positive CLLJ anomalies. This is driven by widely negative β_{CLLJ} coefficients particularly between May-

September (**Figure S3**). Moisture transported from the Caribbean has been identified as the primary moisture source for Central America (Durán-Quesada et al., 2010), where a stronger CLLJ leads to more positive precipitation anomalies on the Caribbean coast of Central America at the jet exit and negative anomalies on the Pacific slopes due to orographic effects, divergence, and subsidence (Magaña et al., 1999; Peña & Douglas, 2002; Taylor et al., 2013). This relationship may be slightly stronger during the full May-October period as it integrates across the full period for which the CLLJ intensifies during the boreal summer (García-Martínez & Bollasina, 2020).

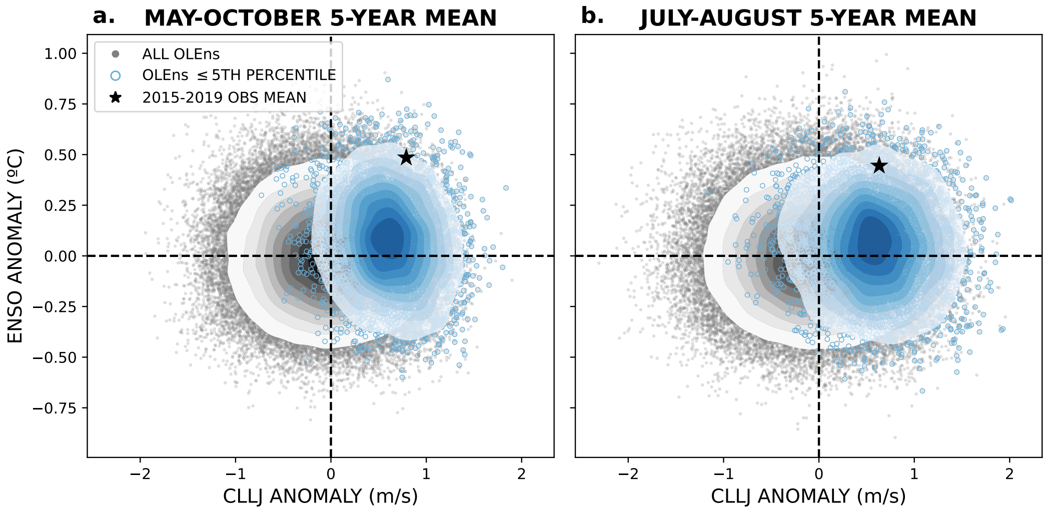

Figure 4. **(a)** Scatter plot of 5-year means of May-October ENSO and CLLJ anomalies for all 5-year prec-synth-OLE periods (grey) and 5-year prec-synth-OLE periods where May-October prec-synth-OLE rainfall is $< 5^{th}$ percentile (blue). Rings represent density of points. The observed 2015-2019 May-October ENSO and CLLJ anomaly is marked with the star. **(b)** Scatter plot of 5-year means of July-August ENSO and CLLJ anomalies for all 5-year prec-synth-OLE periods (grey) and 5-year prec-synth-OLE periods where July-August prec-synth-OLE rainfall is $< 5^{th}$ percentile (blue). Rings represent density of points. The observed 2015-2019 July-August ENSO and CLLJ anomaly is marked with the star.

While the 2015-2019 CLLJ anomaly was the strongest on record, it has not yet been linked to anthropogenic climate change during that period (Pascale et al., 2021). However, future regional drying coincides with simulated shifts in the CLLJ and ENSO that are associated with rainfall deficits in Central America today (Neelin et al., 2006; Rauscher et al., 2011; Karmalkar et al., 2011; Taylor et al., 2013; Fuentes-Franco et al., 2015). Drivers include a southward displacement of the ITCZ and a strengthening and earlier westward movement of the North Atlantic Subtropical High (Neelin et al., 2006; Rauscher et al., 2011). This is coincident with a stronger CLLJ and less warming in the tropical North Atlantic compared to the surrounding oceans (Taylor et al., 2013; Rauscher et al., 2011). A warmer ENSO-like state in the tropical Pacific and enhanced warming relative to the tropical Atlantic can lead to additional rainy season drying (Rauscher et al., 2011; Fuentes-Franco et al., 2015). Despite uncertainties in the magnitude of change and shortcomings in climate models' ability to represent the seasonal cycle of Central American rainfall (Karmalkar et al., 2011; Cavazos et al., 2020), these mechanisms are associated with future drying throughout the CADC.

3.3 The Role of Warming

The PDSI OLEns provides additional information on the compound influences of temperature and precipitation on agricultural drought severity. Similar to the precipitation results, the observed regional PDSI anomaly does not yet fall outside the range of variability produced by the unforced pdsi-synth-OLE (**Figure S4a**). However, the May-October observational PDSI was quite low and falls below the 5^{th} percentile of all 5-year means from the unforced pdsi-synth-OLE. Including the forced term in the pdsi-synth-OLE regression increases the probability of the observed event of equal or greater magnitude; 6.6% of all possible May-October 5-year events are drier than the 2015-2019 event in the forced pdsi-synth-OLE as compared to 4.5% in the unforced pdsi-synth-OLE. This demonstrates that anthropogenic forcing makes soil moisture extremes (as measured by PDSI) and agricultural droughts more likely and expands the distribution to include a wider range of possible PDSI values. These results are consistent with other studies where drought remains dominated by natural rainfall variability, but has been intensified by warming (Griffin & Anchukaitis, 2014; Diffenbaugh et al., 2015; Williams et al., 2015, 2020). Recent research on the Caribbean drought that occurred between 2013 and 2016 also revealed that warming temperatures exacerbated soil moisture deficits and expanded the susceptible area (Herrera et al., 2018). The observed PDSI trend does not yet fall outside the range of natural variability, but including the forced component approximately doubles the chance of occurrence of a negative trend equal to or more negative than the observed trend (**Figure S4b**). Considering the projected precipitation trends for the Central American region, compound hot-dry events will likely become more common in the future (Sarhadi et al., 2018; Bevacqua et al., 2022).

4 Conclusions

Although Central America has experienced significant droughts in the past, the wide-ranging impacts of the 2015-2019 event on ecosystems, agriculture, and livelihoods exposes the need for better understanding the likelihood of severe extended precipitation deficits to improve hazard preparedness and resource management (Pons et al., 2016; Hannah et al., 2017; Hidalgo, 2021). Our capacity to characterize such events, however, is limited in the the absence of long instrumental records and climate model weaknesses in simulating regional precipitation patterns. The statistical OLEns method we use here helps address these gaps, allows us to better characterize the range of possible internal variability, and attends to some of the known climate model limitations. We show that while the 2015-2019 period is the driest 5-year period in the observational record, events of equal or greater magnitude can occur, although very rarely, even without the influence of human-caused climate change. Analysis of subseasonal variations – as indicated by the strong July-August deficits – is critical for understanding the complexity and heterogeneity among individual drought events and their drivers in order to ultimately reduce impacts as events unfold (Hao et al., 2018). The additional influence of temperature as represented in the PDSI OLEns suggests reduced soil moisture is more likely and that the range of possible agricultural drought conditions increases when accounting for anthropogenic warming. Our addition of the Caribbean Low-Level Jet to the OLEns is critical, as it is the mode most directly and strongly associated with dry periods in the region. While natural climate variability remains the dominant signal regionally, continued 21^{st} century warming is projected to lead to increased aridity in Central America (Hidalgo et al., 2019; Hidalgo, 2021). This will make droughts such as the 2015-2019 event more common in the future and require adaptations to meet the challenges presented by shifts in hydroclimate.

5 Data Availability Statement

The original observational large ensemble code is available at `https://github.com/karenamckinnon`. Our adapted observational large ensemble that includes the CLLJ and all data analysis code are available at `https://github.com/taliaanderson`. This includes a netcdf file with all large-scale climate mode time series. The ENSO time series was obtained from `https://www.esrl.noaa.gov/psd/gcos_wgsp/Timeseries/Data/nino34.long.data`. The AMV time series can be found at `https://www.esrl.noaa.gov/psd/data/correlation/amon.us.long.data`. The PDO time series is from `https://www.ncei.noaa.gov/access/monitoring/pdo/`. The two datasets for the CLLJ can be obtained from `psl.noaa.gov/data/gridded/data.20thC_ReanV3.html` and `https://iridl.ldeo.columbia.edu/maproom/ACToday/Colombia/CLLJI.html#tabs-1`. Precipitation data was obtained from `https://opendata.dwd.de/climate_environment/GPCC/html/fulldata-daily_v2020_doi_download.html`. PDSI data is available at `https://crudata.uea.ac.uk/cru/data/drought/`. The CMIP6 data was obtained from `https://climexp.knmi.nl/getindices.cgi?WMO=CMIP6/Tglobal/global_tas_mon_mod_ssp245_192_ave&STATION=CMIP6_ssp245_Tglobal&TYPE=i&id=someone@somewhere`.

Acknowledgments

TGA, DP, and KJA are supported by a grant from the US National Science Foundation (NSF HEGS 2049657). KAM is supported by the Packard Foundation. Our analysis was made possible with the high-performance computing from Cheyenne (doi:10.5065/D6RX99HX) provided by NCAR's Computational and Information Systems Laboratory, supported by the NSF.

References

Aguilar, E., Peterson, T., Obando, P. R., Frutos, R., Retana, J., Solera, M., . . . others (2005). Changes in precipitation and temperature extremes in Central America and northern South America, 1961–2003. *Journal of Geophysical Research: Atmospheres*, *110*(D23).

Alfaro, E. J. (2000). Some characteristics of the precipitation annual cycle in Central America and their relationships with its surrounding tropical oceans. *Top. Meteor. Oceanog*, *7*(2), 99–115.

Almazroui, M., Islam, M. N., Saeed, F., Saeed, S., Ismail, M., Ehsan, M. A., . . . others (2021). Projected changes in temperature and precipitation over the United States, Central America, and the Caribbean in CMIP6 GCMs. *Earth Systems and Environment*, *5*(1), 1–24.

Anchukaitis, K. J., Taylor, M. J., Leland, C., Pons, D., Martin-Fernandez, J., & Castellanos, E. (2015). Tree-ring reconstructed dry season rainfall in Guatemala. *Climate dynamics*, *45*(5-6), 1537–1546.

Anderson, T. G., Anchukaitis, K. J., Pons, D., & Taylor, M. (2019). Multiscale trends in the Central American Midsummer Drought and regional precipitation extremes. *Environmental Research Letters*, *14*.

Barichivich, J., Osborn, T. J., Harris, I., van der Schrier, G., & Jones, P. (2022). Monitoring global drought using the self-calibrating Palmer Drought Severity Index.

Beguería, S., Vicente-Serrano, S. M., Tomás-Burguera, M., & Maneta, M. (2016). Bias in the variance of gridded data sets leads to misleading conclusions about changes in climate variability. *International Journal of Climatology*, *36*(9), 3413–3422.

Bevacqua, E., Zappa, G., Lehner, F., & Zscheischler, J. (2022). Precipitation trends determine future occurrences of compound hot–dry events. *Nature Climate Change*, *12*(4), 350–355.

Box, G. E., & Cox, D. R. (1964). An analysis of transformations. *Journal of the*

Royal Statistical Society: Series B (Methodological), *26*(2), 211–243.
Cavazos, T., Luna-Niño, R., Cerezo-Mota, R., Fuentes-Franco, R., Méndez, M., Pineda Martinez, L. F., & Valenzuela, E. (2020). Climatic trends and regional climate models intercomparison over the CORDEX-CAM (Central America, Caribbean, and Mexico) domain. *International Journal of Climatology*, *40*(3), 1396–1420.
CONASAN. (2014). *Informe Daños Ocasionados por la Canícula Prolongada 2014* (Tech. Rep.). CONASAN.
Cook, B. I., Mankin, J., Marvel, K., Williams, A., Smerdon, J., & Anchukaitis, K. (2020). Twenty-First Century Drought Projections in the CMIP6 Forcing Scenarios. *Earth's Future*, *8*(6), e2019EF001461.
Cook, B. I., Mankin, J. S., & Anchukaitis, K. J. (2018). Climate change and drought: From past to future. *Current Climate Change Reports*, *4*, 164–179.
Dai, A., Fyfe, J. C., Xie, S.-P., & Dai, X. (2015). Decadal modulation of global surface temperature by internal climate variability. *Nature Climate Change*, *5*(6), 555–559.
Depsky, N., & Pons, D. (2020). Meteorological droughts are projected to worsen in Central America's Dry Corridor throughout the 21st century. *Environmental Research Letters*, *16*(1), 014001.
Deser, C. (2020). Certain uncertainty: The role of internal climate variability in projections of regional climate change and risk management. *Earth's Future*, *8*(12), e2020EF001854.
Deser, C., Phillips, A. S., Alexander, M. A., & Smoliak, B. V. (2014). Projecting North American climate over the next 50 years: Uncertainty due to internal variability. *Journal of Climate*, *27*(6), 2271–2296.
Diffenbaugh, N. S., Swain, D. L., & Touma, D. (2015). Anthropogenic warming has increased drought risk in California. *Proceedings of the National Academy of Sciences*, *112*(13), 3931–3936.
Durán-Quesada, A. M., Gimeno, L., Amador, J., & Nieto, R. (2010). Moisture sources for Central America: Identification of moisture sources using a Lagrangian analysis technique. *Journal of Geophysical Research: Atmospheres*, *115*(D5).
Eyring, V., Bony, S., Meehl, G. A., Senior, C. A., Stevens, B., Stouffer, R. J., & Taylor, K. E. (2016). Overview of the Coupled Model Intercomparison Project Phase 6 (CMIP6) experimental design and organization. *Geoscientific Model Development*, *9*(5), 1937–1958.
Food and Agriculture Organization. (2015). *Disaster Risk Programme to strengthen resilience in the Dry Corridor in Central America* (Tech. Rep.). FAO.
Food and Agriculture Organization (FAO). (2018, August). *FAO and WFP concerned about the impact of drought on the most vulnerable in Central America.* FAO (News Release).
Fuentes-Franco, R., Coppola, E., Giorgi, F., Pavia, E. G., Diro, G. T., & Graef, F. (2015). Inter-annual variability of precipitation over Southern Mexico and Central America and its relationship to sea surface temperature from a set of future projections from CMIP5 GCMs and RegCM4 CORDEX simulations. *Climate Dynamics*, *45*(1-2), 425–440.
García-Martínez, I. M., & Bollasina, M. A. (2020). Sub-monthly evolution of the Caribbean Low-Level Jet and its relationship with regional precipitation and atmospheric circulation. *Climate Dynamics*, *54*(9), 4423–4440.
Giannini, A., Cane, M. A., & Kushnir, Y. (2001). Interdecadal changes in the ENSO teleconnection to the Caribbean region and the North Atlantic Oscillation. *Journal of Climate*, *14*(13), 2867–2879.
Giannini, A., Kushnir, Y., & Cane, M. A. (2000). Interannual variability of Caribbean rainfall, ENSO, and the Atlantic Ocean. *Journal of Climate*, *13*(2), 297–311.

Gotlieb, Y., Pérez-Briceño, P. M., Hidalgo, H., & Alfaro, E. (2019). The Central American Dry Corridor: a consensus statement and its background. *Revista Mesoamericana de Biodiversidad y Cambio Climático*, *3*(5), 42–51.

Griffin, D., & Anchukaitis, K. J. (2014). How unusual is the 2012–2014 California drought? *Geophysical Research Letters*, *41*(24), 9017–9023.

Hannah, L., Donatti, C. I., Harvey, C. A., Alfaro, E., Rodriguez, D. A., Bouroncle, C., … others (2017). Regional modeling of climate change impacts on smallholder agriculture and ecosystems in Central America. *Climatic Change*, *141*(1), 29–45.

Hao, Z., Singh, V. P., & Xia, Y. (2018). Seasonal drought prediction: advances, challenges, and future prospects. *Reviews of Geophysics*, *56*(1), 108–141.

Hastenrath, S., & Polzin, D. (2012). Climatic variations in Central America and the Caribbean. *International Journal of Climatology*, *33*(6), 1348–1356.

Herrera, D. A., Ault, T. R., Fasullo, J. T., Coats, S. J., Carrillo, C. M., Cook, B. I., & Williams, A. P. (2018). Exacerbation of the 2013–2016 pan-Caribbean drought by anthropogenic warming. *Geophysical Research Letters*, *45*(19), 10–619.

Hidalgo, H. G. (2021). Climate variability and change in Central America: what does it mean for water managers? *Frontiers in Water*, 81.

Hidalgo, H. G., Alfaro, E. J., Amador, J. A., & Bastidas, Á. (2019). Precursors of quasi-decadal dry-spells in the Central America Dry Corridor. *Climate Dynamics*, *53*(3), 1307–1322.

Hidalgo, H. G., Durán-Quesada, A. M., Amador, J. A., & Alfaro, E. J. (2015). The Caribbean Low-Level Jet, the Inter-Tropical Convergence Zone and Precipitation Patterns in the Intra-Americas Sea: A Proposed Dynamical Mechanism. *Geografiska Annaler: Series A, Physical Geography*, *97*(1), 41–59.

Huang, B., Thorne, P. W., Banzon, V. F., Boyer, T., Chepurin, G., Lawrimore, J. H., … Zhang, H.-M. (2017). Extended reconstructed sea surface temperature, version 5 (ERSSTv5): upgrades, validations, and intercomparisons. *Journal of Climate*, *30*(20), 8179–8205.

Hussain, M., & Mahmud, I. (2019). pyMannKendall: a python package for non parametric Mann Kendall family of trend tests. *Journal of Open Source Software*, *4*(39), 1556.

Jones, P. D., Harpham, C., Harris, I., Goodess, C. M., Burton, A., Centella-Artola, A., … others (2016). Long-term trends in precipitation and temperature across the Caribbean. *International Journal of Climatology*, *36*(9), 3314–3333.

Kalnay, E., Kanamitsu, M., Kistler, R., Collins, W., Deaven, D., Gandin, L., … others (1996). The NCEP/NCAR 40-year reanalysis project. *Bulletin of the American meteorological Society*, *77*(3), 437–472.

Kaplan, A., Cane, M. A., Kushnir, Y., Clement, A. C., Blumenthal, M. B., & Rajagopalan, B. (1998). Analyses of global sea surface temperature 1856–1991. *Journal of Geophysical Research: Oceans*, *103*(C9), 18567–18589.

Karmalkar, A. V., Bradley, R. S., & Diaz, H. F. (2011, May). Climate change in Central America and Mexico: regional climate model validation and climate change projections. *Climate Dynamics*, *37*(3-4), 605–629. Retrieved from `http://dx.doi.org/10.1007/s00382-011-1099-9` doi: 10.1007/s00382-011-1099-9

Karnauskas, K. B., & Busalacchi, A. J. (2009). The role of SST in the east Pacific warm pool in the interannual variability of Central American rainfall. *Journal of Climate*, *22*(10), 2605–2623.

Lehner, F., Deser, C., Maher, N., Marotzke, J., Fischer, E. M., Brunner, L., … Hawkins, E. (2020). Partitioning climate projection uncertainty with multiple large ensembles and CMIP5/6. *Earth System Dynamics*, *11*(2), 491–508.

Magaña, V., Amador, J. A., & Medina, S. (1999). The midsummer drought over Mexico and Central America. *Journal of Climate*, *12*(6), 1577–1588.

Mankin, J. S., Lehner, F., Coats, S., & McKinnon, K. A. (2020). The value of initial condition large ensembles to robust adaptation decision-making. *Earth's Future*, *8*(10), e2012EF001610.

Mantua, N. J., & Hare, S. R. (2002). The Pacific Decadal Oscillation. *Journal of oceanography*, *58*, 35–44.

Masson-Delmotte, V., Zhai, P., Pirani, S., Connors, C., Péan, S., Berger, N., ... Scheel Monteiro, P. M. (2021). IPCC, 2021: Summary for Policymakers. In: Climate change 2021: The Physical Science Basis. Contribution of Working Group I to the Sixth Assessment Report of the Intergovernmental Panel on Climate Change.

Maurer, E. P., Roby, N., Stewart-Frey, I. T., & Bacon, C. M. (2017). Projected twenty-first-century changes in the Central American mid-summer drought using statistically downscaled climate projections. *Regional Environmental Change*, *17*(8), 2421–2432.

Maurer, E. P., Stewart, I. T., Joseph, K., & Hidalgo, H. G. (2022). The Mesoamerican mid-summer drought: the impact of its definition on occurrences and recent changes. *Hydrology and Earth System Sciences*, *26*(5), 1425–1437.

McKinnon, K. A., & Deser, C. (2018). Internal variability and regional climate trends in an observational large ensemble. *Journal of Climate*, *31*(17), 6783–6802.

McKinnon, K. A., & Deser, C. (2021). The inherent uncertainty of precipitation variability, trends, and extremes due to internal variability, with implications for Western US water resources. *Journal of Climate*, *34*(24), 9605–9622.

McKinnon, K. A., Poppick, A., Dunn-Sigouin, E., & Deser, C. (2017). An "observational large ensemble" to compare observed and modeled temperature trend uncertainty due to internal variability. *Journal of Climate*, *30*(19), 7585–7598.

Morton, J. F. (2007). The impact of climate change on smallholder and subsistence agriculture. *Proceedings of the national academy of sciences*, *104*(50), 19680–19685.

Muñoz-Jiménez, R., Giraldo-Osorio, J. D., Brenes-Torres, A., Avendaño-Flores, I., Nauditt, A., Hidalgo-León, H. G., & Birkel, C. (2019). Spatial and temporal patterns, trends and teleconnection of cumulative rainfall deficits across Central America. *International Journal of Climatology*, *39*(4), 1940–1953.

Neelin, J. D., Münnich, M., Su, H., Meyerson, J. E., & Holloway, C. E. (2006). Tropical drying trends in global warming models and observations. *Proceedings of the National Academy of Sciences*, *103*(16), 6110–6115.

O'Neill, B. C., Tebaldi, C., Van Vuuren, D. P., Eyring, V., Friedlingstein, P., Hurtt, G., ... others (2016). The scenario model intercomparison project (ScenarioMIP) for CMIP6. *Geoscientific Model Development*, *9*(9), 3461–3482.

Pascale, S., Kapnick, S. B., Delworth, T. L., Hidalgo, H. G., & Cooke, W. F. (2021). Natural variability vs forced signal in the 2015–2019 Central American drought. *Climatic Change*, *168*(3), 1–21.

Peña, M., & Douglas, M. W. (2002). Characteristics of wet and dry spells over the Pacific side of Central America during the rainy season. *Monthly Weather Review*, *130*(12), 3054–3073.

Pons, D., Taylor, M. J., Griffin, D., Castellanos, E. J., & Anchukaitis, K. J. (2016, Nov). On the Production of Climate Information in the High Mountain Forests of Guatemala. *Annals of the American Association of Geographers*, *107*(2), 323–335. doi: 10.1080/24694452.2016.1235481

Rauscher, S. A., Giorgi, F., Diffenbaugh, N. S., & Seth, A. (2008, Feb). Extension and Intensification of the Meso-American mid-summer drought in the twenty-first century. *Climate Dynamics*, *31*(5), 551–571. doi: 10.1007/s00382-007-0359-1

Rauscher, S. A., Kucharski, F., & Enfield, D. B. (2011). The role of regional SST warming variations in the drying of Meso-America in future climate projec-

tions. *Journal of Climate*, *24*(7), 2003–2016.
Rayner, N., Parker, D. E., Horton, E., Folland, C. K., Alexander, L. V., Rowell, D., ... Kaplan, A. (2003). Global analyses of sea surface temperature, sea ice, and night marine air temperature since the late nineteenth century. *Journal of Geophysical Research: Atmospheres*, *108*(D14).
Sarhadi, A., Ausín, M. C., Wiper, M. P., Touma, D., & Diffenbaugh, N. S. (2018). Multidimensional risk in a nonstationary climate: Joint probability of increasingly severe warm and dry conditions. *Science Advances*, *4*(11), eaau3487.
Schneider, U., Becker, A., Finger, P., Rustemeier, E., & Ziese, M. (2020). GPCC Full Data Monthly Product Version 2020 at 0.5 °: Monthly Land-Surface Precipitation from Rain-Gauges built on GTS-based and Historical Data.
Schneider, U., Finger, P., Meyer-Christoffer, A., Rustemeier, E., Ziese, M., & Becker, A. (2017). Evaluating the hydrological cycle over land using the newly-corrected precipitation climatology from the Global Precipitation Climatology Centre (GPCC). *Atmosphere*, *8*(3), 52.
Schreiber, T., & Schmitz, A. (1996). Improved surrogate data for nonlinearity tests. *Physical review letters*, *77*(4), 635.
Stewart, I. T., Maurer, E. P., Stahl, K., & Joseph, K. (2021). Recent evidence for warmer and drier growing seasons in climate sensitive regions of Central America from multiple global datasets. *International Journal of Climatology*.
Taylor, M. A., & Alfaro, E. J. (2005). Climate of Central America and the Caribbean. *Encyclopedia of world climatology*, 183–189.
Taylor, M. A., Whyte, F. S., Stephenson, T. S., & Campbell, J. D. (2013). Why dry? Investigating the future evolution of the Caribbean low level jet to explain projected Caribbean drying. *International Journal of Climatology*, *33*(3), 784–792.
The World Food Programme (WFP). (2019, April). *Erratic weather patterns in the Central American Dry Corridor leave 1.4 million people in urgent need of food assistance.* WFP (News Release).
Thompson, D. W., Barnes, E. A., Deser, C., Foust, W. E., & Phillips, A. S. (2015). Quantifying the role of internal climate variability in future climate trends. *Journal of Climate*, *28*(16), 6443–6456.
United Nations. (2018, August). *Central America: drought, resulting crop losses threaten food security of two million people, UN warns.* UN (News Release).
United Nations Office for the Coordination of Humanitarian Affairs. (2017). *Central America: Drought - 2014-2017* (Tech. Rep.). OCHA.
van der Schrier, G., Barichivich, J., Briffa, K., & Jones, P. (2013). A scPDSI-based global data set of dry and wet spells for 1901–2009. *Journal of Geophysical Research: Atmospheres*, *118*(10), 4025–4048.
Van der Zee Arias, A., Meyrat, A., Picado, L., Poveda, C., & Van der Zee, J. (2012). *Estudio de caracterización del corredor seco centroamericano* (Tech. Rep.). FAO.
Wang, C. (2007). Variability of the Caribbean low-level jet and its relations to climate. *Climate dynamics*, *29*(4), 411–422.
Wilks, D. S. (1997). Resampling hypothesis tests for autocorrelated fields. *Journal of Climate*, *10*(1), 65–82.
Williams, A. P., Cook, E. R., Smerdon, J. E., Cook, B. I., Abatzoglou, J. T., Bolles, K., ... Livneh, B. (2020). Large contribution from anthropogenic warming to an emerging North American megadrought. *Science*, *368*(6488), 314–318.
Williams, A. P., Seager, R., Abatzoglou, J. T., Cook, B. I., Smerdon, J. E., & Cook, E. R. (2015). Contribution of anthropogenic warming to California drought during 2012–2014. *Geophysical Research Letters*, *42*(16), 6819–6828.
Yue, S., & Wang, C. Y. (2002). Applicability of prewhitening to eliminate the influence of serial correlation on the Mann-Kendall test. *Water resources research*, *38*(6), 4–1.